Recent R Measurement at BES

Ping Wang

BES Collaboration

PHIPSI08

Laboratori Nazionali di Frascati, Italy

Outline

- R value in continuous region
- High mass charmonia parameters

What is R value

By definition

$$R = \frac{\sigma^0_{had}(e^+e^- \to \gamma^* \to \mathrm{hadrons})}{\sigma^0_{\mu\mu}(e^+e^- \to \gamma^* \to \mu^+\mu^-)}$$

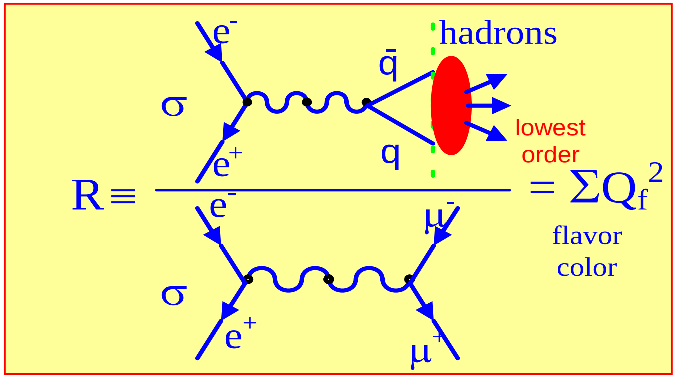

R value is the inclusive hadronic cross section in e^+e^- annihilation normalized by Born cross section of $\mu^+\mu^-$.

Significances: error of R value has important influence upon the precise test of the Standard Model (SM), such as calculation of the running electromagnetic coupling constant $\alpha(s)$, anomalous μ magnetic moment (g-2), global fit of the Higgs mass, direct test to the pQCD prediction on R_{QCD} (s).

below 5 GeV, use data

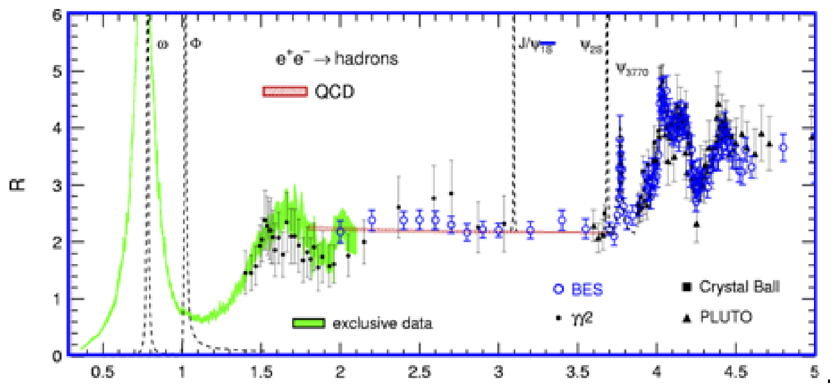

above 5 GeV, use pQCD

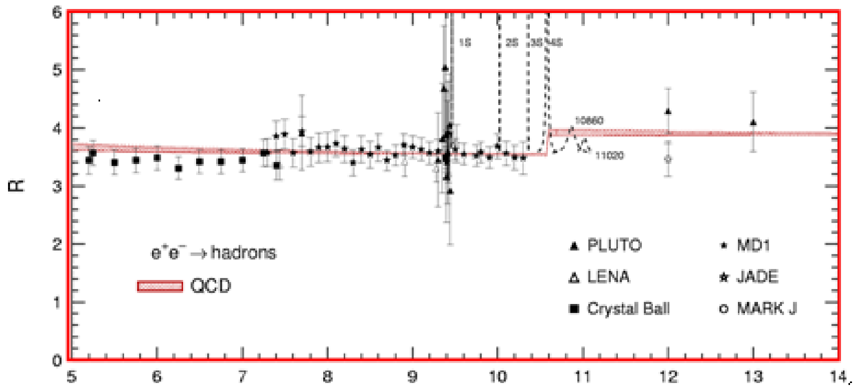

R expression in experiment

R value is measured by

$$\boxed{R_{exp} = \frac{N_{had}^{obs} - N_{bg}}{\sigma_{\mu\mu}^{0} L \epsilon_{trg} \epsilon_{had}^{0} (1 + \delta_{obs})}}$$

N_{had}^{obs} **: number of hadronic events;**

N_{bg} **: number of background events;** L **: integrated luminosity;**

ϵ_{trg} **: trigger efficiency;** ϵ_{had}^{0} **: hadronic efficiency;**

$(1 + \delta_{obs})$ **: effective ISR correction factor.**

In expression R_{exp}, each quantity is obtained by

- data analysis $\longrightarrow$ N_{had}^{obs} N_{bg} L ϵ_{trg}
- theoretical calculations $\longrightarrow$ $(1 + \delta_{obs})$
- Monte Carlo simulations $\longrightarrow$ ϵ_{had}^{0}

Previous measurements

- In 1998 & 1999, scan data were taken between 2-5 GeV
- Energy step: in 3.7– 5.0 GeV are 10–20MeV, elsewhere is 100MeV
- Generation simulation: tuned LUARLW and JETSET
- Detector simulation: software based on EGS4
- Event selection: hadronic events with $N_{had} \geq$ 2-prong are selected
- Statistic error: about 2~3 %
- Systematic error: about 5~8 % (event selection and efficiency are dominant)
- Results: PRL 84 (2000) 594, PRL 88 (2002) 101802

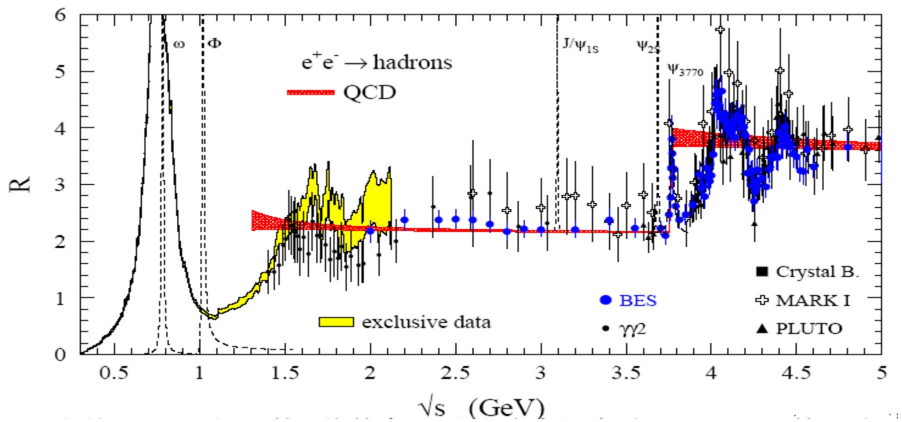

Present measurement

- **In 2004, data at** 2.20**,** 2.6**0,** 3.07 **and** 3.65 GeV **were taken**
- **Statistical error:** small, about 0.5%
- **Generation simulation:** LUARLW is retuned with improved way
- **Detector simulation:** is updated by GEANT3 based software
- **Event selection:** improved, $N_{\mathrm{had}} \geq$ 1-prong events are selected
- **Systematical error:** about 3.3%

Integral luminosity

$\sqrt{s}$ (GeV)	L (nb^{-1})	$\Delta L/L$ (%)
2.200	121.50±1.10±4.00	3.41
2.600	1215.98±4.08±23.96	2.00
3.070	2272.20±6.64±30.00	1.35
3.650	6456.83±13.24±87.81	1.38

Observed number of hadronic events

$N_{had}^{obs}(N_{gd} \geq 1\text{-prong})$	$N_{had}^{obs}(N_{gd} \geq 2\text{-prong})$
2862	2480
24026	21511
33933	31063
83767	77660

Effective ISR correction

Radiative correction:

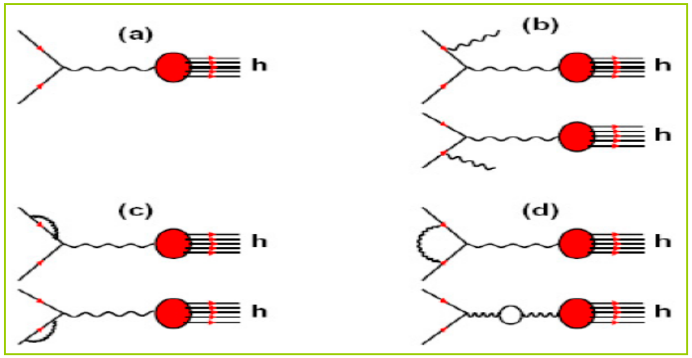

References:

G.Bonneau Nucl. Phys. B27, (1971) 281-397

F.A.Berends Nucl. Phys. B178, (1981)141-150

A.Osterfeld SLAC-PUB-4160(1986)

precision is ~ 1% for $O(\alpha^3)$, it agrees Kureav & Fadin's calculation within ~1%

Observed total hadronic cross section:

$$\sigma^T_{obs} = \frac{N_{had}}{L}$$

R value may be measured by

Procedure A: $\sigma^T = \frac{\sigma^T_{obs}}{\bar{\epsilon}} \quad \Rightarrow \quad R = \frac{N_{had}}{\sigma^0_{\mu\mu} L \bar{\epsilon}(1+\delta)}$

or

Procedure B: $\sigma^0_{obs} = \frac{\sigma^T_{obs}}{1+\delta_{obs}} \quad \Rightarrow \quad R = \frac{N_{had}}{\sigma^0_{\mu\mu} L \epsilon(0)(1+\delta_{obs})}$ √

$(1+\delta)$ and $(1+\delta_{obs})$ are theoretical and effective ISR correction factors

$\bar{\epsilon}$ and $\epsilon(0)$ are efficiencies with and without radiation

Lund area law

Hadronization picture :

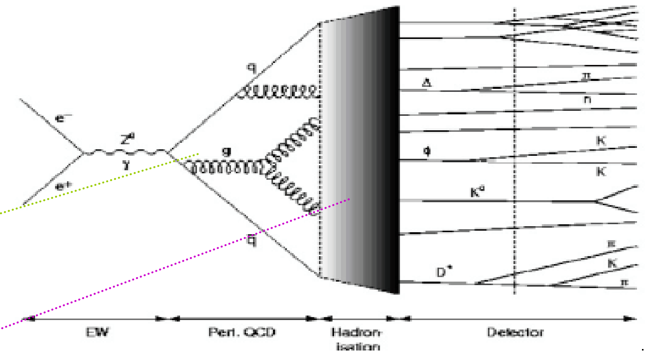

Hadron production via string fragmentation:

$$e^+e^- \Rightarrow q\bar{q} \Rightarrow \text{string} \Rightarrow m_1 + m_2 + \cdots + m_n$$

Effective matrix element (gluon emission is neglected)

$$\mathcal{M} \equiv \mathcal{M}_{\text{QED}}(e^+e^- \longrightarrow q\bar{q})\mathcal{M}_{\text{LUND}}(q\bar{q} \longrightarrow m_1, m_2, \cdots m_n)$$

String fragmentation:

$$\mathcal{M}_{\text{LUND}}(q\bar{q} \longrightarrow m_1, m_2, \cdots m_n) = C_n \mathcal{M}_{\perp} \mathcal{M}_{//}$$

Transverse momentum (Gaussian) $\mathcal{M}_{\perp} = \exp(-\sum_{j}^{n} \vec{k}_j^{\,2})$ $\quad \vec{k}_j \equiv \dfrac{\vec{p}_{\perp j}}{2\sigma}$

Longitudinal momentum (Lund area law):

$$\mathcal{M}_{//} = \exp(i\xi\mathcal{A}_n) \qquad \xi = \frac{1}{2\kappa} + i\frac{b}{2}$$

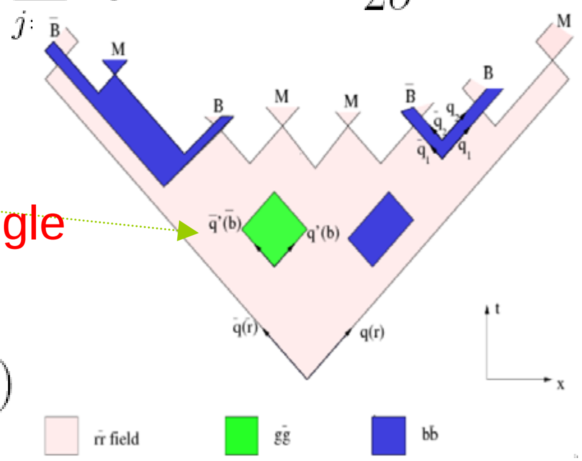

Simulation of ISR has been built in LUARLW with the angle and momentum distributions

$$d\sigma^{HB}(s) = \frac{\alpha}{\pi^2}\frac{\sin^2\theta}{(1-a^2\cos^2\theta)}\frac{dk\,d\Omega_\gamma}{k}(1-k+\frac{k^2}{2})d\sigma^0(s')$$

Comparisons between data and LUARLW

@ 3.65 GeV

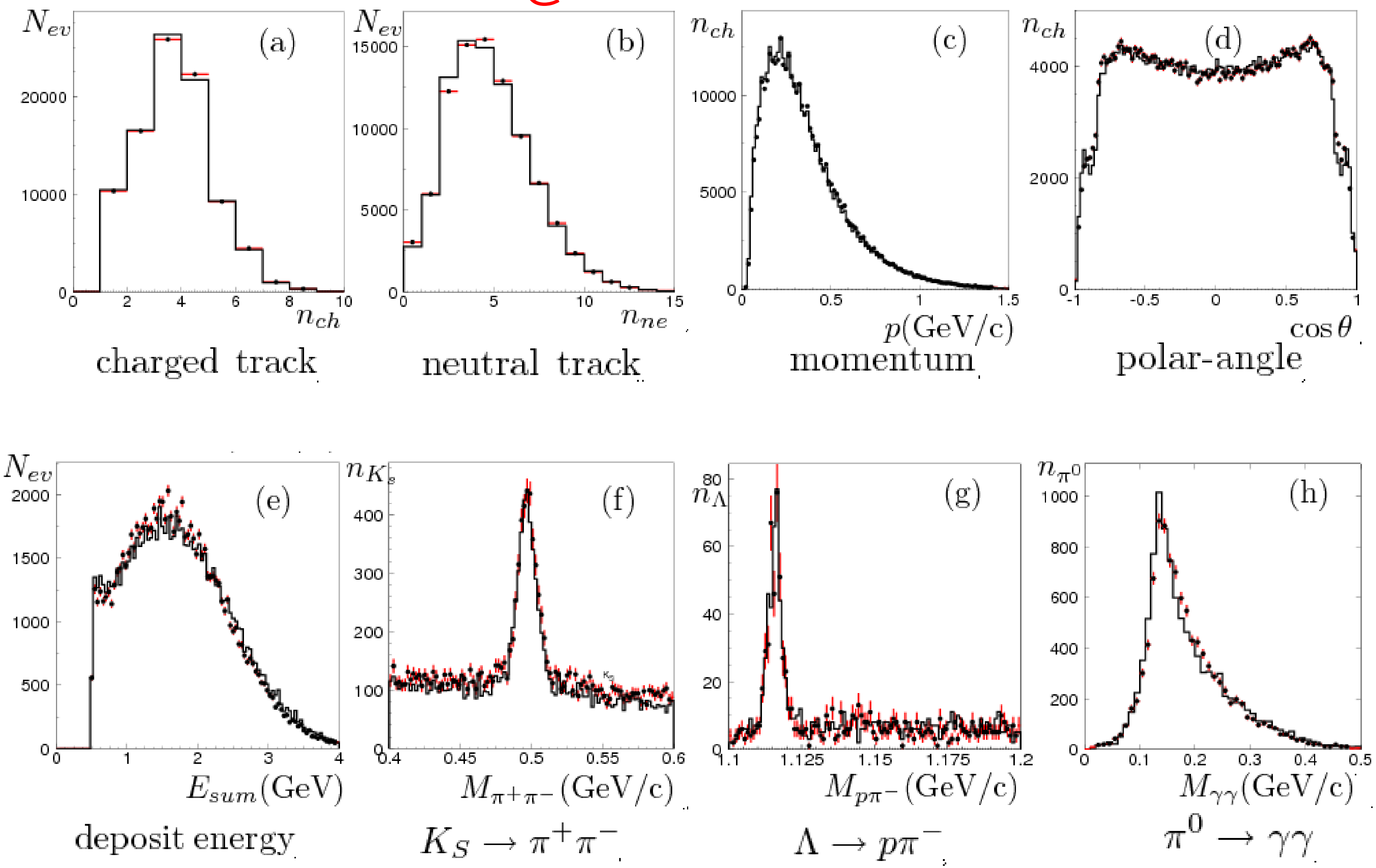

Error analysis

According to experimental expression

$$R_{exp} = \frac{N_{had}^{obs}}{\sigma_{\mu\mu}^{0} L \epsilon_{trg} \bar{\epsilon}_{had} (1+\delta)}$$

the effective number of hadronic events is defined

$$\tilde{N}_{had} = \frac{N_{had}}{\bar{\epsilon}_{had}} \quad , \text{ where } \quad \bar{\epsilon}_{hd} = \frac{N_{obs}^{MC}}{N_{gen}^{MC}}$$

Main error estimation:

$$\frac{\Delta R}{R} \cong \sqrt{\left(\frac{\Delta \tilde{N}_{had}}{\tilde{N}_{had}}\right)^2 + \left(\frac{\Delta L}{L}\right)^2 + \left(\frac{\Delta \epsilon_{trg}}{\epsilon_{trg}}\right)^2 + \left(\frac{\Delta(1+\delta)}{(1+\delta)}\right)^2}$$

Extra error from the track reconstruction

$$\Delta\epsilon_{trk} = \sum_{n_{ch}\geq 1} P(n_{ch}) B(n_{er}; n_{ch}, \sigma_{trk})$$

P **:** multiplicity distribution

B **:** binominal distribution

$\boldsymbol{\sigma_{trk}}$ **:** tracking error (2%)

$\boldsymbol{n_{ch}}$ **:** number of charged track in one event

$\boldsymbol{n_{er}}$ **:** number of wrongly reconstructed tracks in one event

Error $\Delta\varepsilon_{trk}$ due to tracking efficiency (%)

2.200	0.35
2.600	0.32
3.070	0.29
3.650	0.26

Errors of the effective number of hadronic events

(including event selection and hadronic efficiency)

Selection type		Cut condition	Systematic error of $\Delta N_{had}/N_{had}$ (%)			
			2.2 GeV	2.6 GeV	3.07 GeV	3.65 GeV
track level	charged	Mfit=2	0.20	0.24	0.36	0.37
		$V_{xy} < 2$ (cm)	0.45	0.15	0.40	0.90
		$\|cos\theta\| < 0.84$	1.13	0.75	0.78	1.21
		$p < E_b(1 + 0.1\sqrt{1 + E_b^2})$	0.05	0.02	0.02	0.01
		$t_{tof} \le t_{proton} + 2$(ns)	0.06	0.05	0.09	0.13
		$E_{BSC} \le Min(1, 0.6E_b)$	0.67	1.01	0.92	0.64
	neutral	—	—	—	—	—
event level	all tracks	$E_{BSC}^{sum} > Max(0.5, 0.28E_b)$	0.96	0.50	0.74	1.10
	≥3-prong	$N_{good} \ge 3$	—	—	—	—
	=2-prong	$N_{good} = 2$	—	—	—	—
		$\theta_{12} < 165°$	0.87	0.90	0.62	0.54
		$\|\Delta R\| \ge 34$ or $\|\Delta Z\| \ge 60$ (cm)	0.92	0.83	0.87	0.65
	=1-prong	$N_{good} = 1$	—	—	—	—
		if $Xrat_e > 0.5 \to e$	0.63	0.18	0.03	0.15
		if $p > 1$ GeV, $\mu_{hit} \ge 1 \to \mu$	0.19	0.04	0.02	0.14
		$N_\gamma \ge 2$	0.12	0.01	0.01	0.18
		$E_\gamma > 0.1$ GeV	0.97	0.18	0.13	0.40
		$N_{hit\ layer} \ge 2$	0.51	0.14	0.11	0.07
		$\theta_{\gamma chgtrk} > 25°$	0.62	0.68	0.20	0.66
		1-C fit, $Prob(\chi^2) > 0.01$ for π^0	0.40	0.50	0.12	0.09
		Total error for $\Delta N_{had}/N_{had}$	2.58	2.05	1.88	2.33

new

Preliminary results

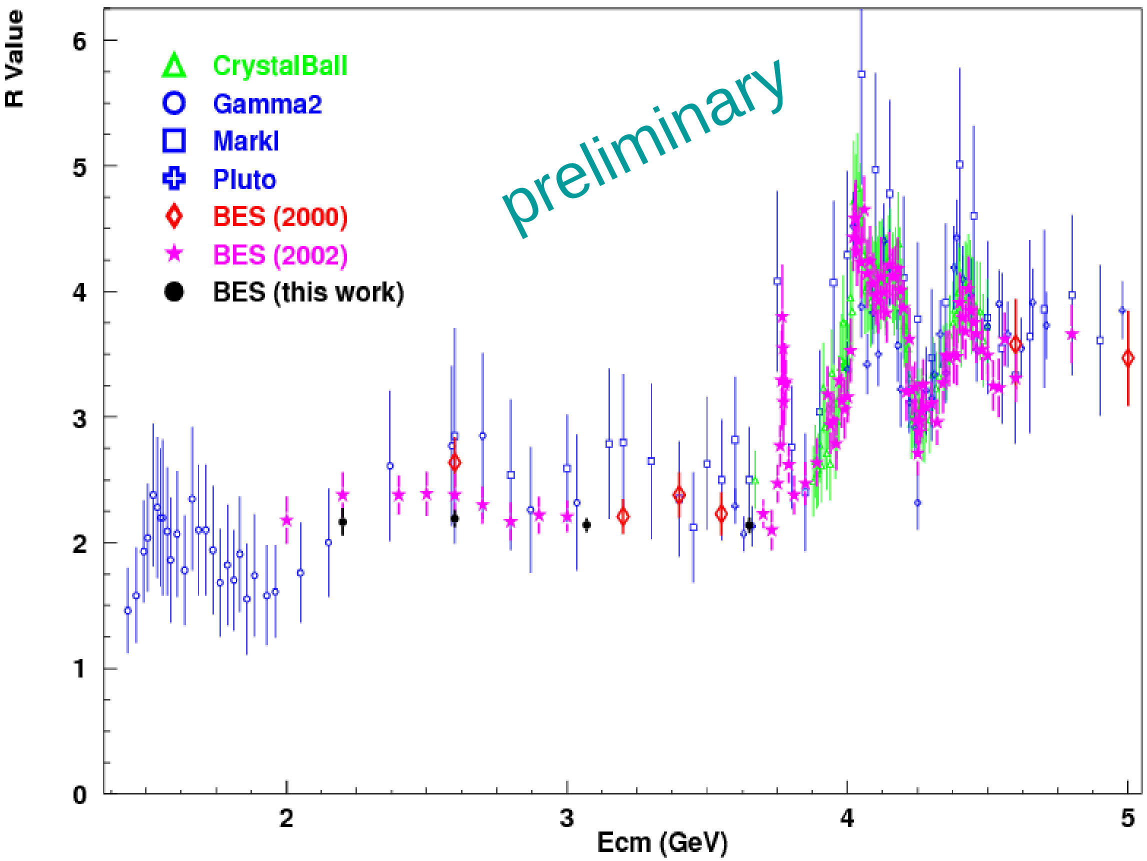

Results show:

- Precisions of new measurements are about 4.8% at 2.20 GeV, and 3.3% at 2.60, 3.07 and 3.65 GeV.
- Values of R for selecting more than 1-prong and 2-prong events are in good consistency.
- The cross checks of R values measured with the procedure A and B are done, their differences are about 1%.

R values measured with procedure B

$\sqrt{s}$(GeV)	$R(N_{gd} \geq$ 1-prong)	$R(N_{gd} \geq$ 2-prong)
2.200	$2.17 \pm 0.04 \pm 0.10$	$2.17 \pm 0.04 \pm 0.10$
2.600	$2.19 \pm 0.01 \pm 0.07$	$2.20 \pm 0.02 \pm 0.07$
3.070	$2.14 \pm 0.01 \pm 0.05$	$2.15 \pm 0.01 \pm 0.06$
3.650	$2.14 \pm 0.01 \pm 0.06$	$2.16 \pm 0.01 \pm 0.06$

Procedure A:

$$R = \frac{N_{had}}{\sigma^0_{\mu\mu} L \bar{\epsilon} (1+\delta)}$$

Procedure B:

$$R = \frac{N_{had}}{\sigma^0_{\mu\mu} L \epsilon(0) (1+\delta_{obs})}$$

Fitting of heavy charmonia parameters

The 4 heavy charmonia with $J^{PC} = 1^{--}$ are

$$\psi(3770) \quad \psi(4040) \quad \psi(4160) \quad \psi(4415)$$

Their properties are characterized by the Breit-Wigner amplitude and resonant parameters:

$$\mathcal{T} = \frac{M\sqrt{\Gamma^e\Gamma^h}}{W^2 - M^2 + iM\Gamma_{tot}} e^{i\delta}$$

- nominal mass M
- total width $\Gamma_{\rm tot}$
- electronic width Γ_{ee}
- initial phase angle δ

According to Eichten's model, there are following decay channels (f)

$$\begin{aligned}
\psi(3770) &\Rightarrow D\bar{D};\\
\psi(4040) &\Rightarrow D\bar{D}, D^*\bar{D}^*, D\bar{D}^*, \bar{D}D^*, D_s\bar{D}_s;\\
\psi(4160) &\Rightarrow D\bar{D}, D^*\bar{D}^*, D\bar{D}^*, \bar{D}D^*, D_s\bar{D}_s, D_s\bar{D}_s^*;\\
\psi(4415) &\Rightarrow D\bar{D}, D^*\bar{D}^*, D\bar{D}^*, \bar{D}D^*, D_s\bar{D}_s, D_s\bar{D}_s^*, D_s^*\bar{D}_s^*.
\end{aligned}$$

K. Seth's results PRD72(2005)017501

K. Seth fitted R values measured by CB and BES, and obtained the resonance parameters of ψ(4040), ψ(4160) and ψ(4415). The values of parameters were updated in PDG2006 mainly based on K. Seth's evaluation.

		$M^{(1)}$ (MeV)	$\Gamma^{(1)}_{tot}$ (MeV)	$\Gamma^{(1)}_{ee}$ (keV)
$\psi(4040)$	PDG[1]	4040 ± 10	52 ± 10	0.75 ± 0.15
	CB[6]	4037 ± 2	85 ± 10	0.88 ± 0.11
	BES[7]	4040 ± 1	89 ± 6	0.91 ± 0.13
	CB+BES	4039.4 ± 0.9	88 ± 5	0.89 ± 0.08
		$M^{(2)}$	$\Gamma^{(2)}_{tot}$	$\Gamma^{(2)}_{ee}$
$\psi(4160)$	PDG[1]	4159 ± 20	78 ± 20	0.77 ± 0.23
	CB[6]	4151 ± 4	107 ± 10	0.83 ± 0.08
	BES[7]	4155 ± 5	107 ± 16	0.84 ± 0.13
	CB+BES	4153 ± 3	107 ± 8	0.83 ± 0.07
		$M^{(3)}$	$\Gamma^{(3)}_{tot}$	$\Gamma^{(3)}_{ee}$
$\psi(4415)$	PDG[1]	4415 ± 6	43 ± 15	0.47 ± 0.10
	CB[6]	4425 ± 6	119 ± 16	0.72 ± 0.11
	BES[7]	4429 ± 9	118 ± 35	0.64 ± 0.23
	CB+BES	4426 ± 5	119 ± 15	0.71 ± 0.10

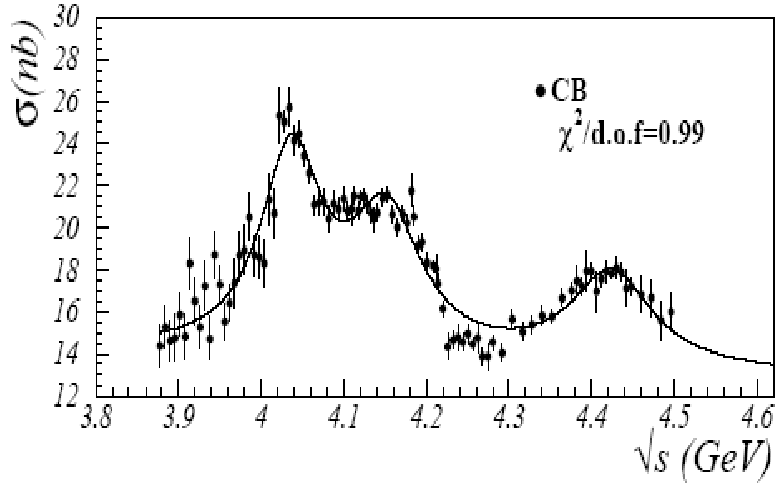

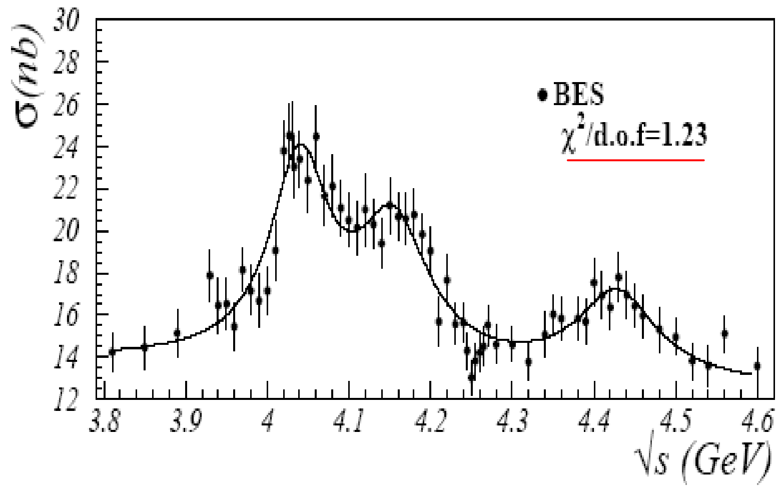

Conclusion:

CB and BES measurements are in excellent agreement

Breit - Wigner amplitude

- **In quantum mechanics, wave function for a unstable particle**

$$\psi(t) = \psi(0)e^{-i\omega t}e^{-t/2\tau} = |\psi(0)|e^{i\delta}e^{-it(M-i\Gamma/2)}$$

initial phase factor
at moment of production

- **The amplitude as the function of energy *W* is**

$$\chi_r(W) = \int \psi_r(t)e^{iWt}dt = \frac{K_r \cdot e^{i\delta_r}}{(W-M_r) - i\Gamma_r/2}$$

- **Usually, Breit-Wigner amplitude is written as**

$$\mathcal{T}_r = \frac{\frac{1}{2}\Gamma_r\ e^{i\delta_r}}{W - M_r - i\Gamma_r/2} = \frac{\frac{1}{2}\sqrt{\Gamma_r \cdot \Gamma_r}\ e^{i\delta_r}}{W - M_r - i\Gamma_r/2}$$

- **If we consider a special process with initial state e^+e^- and decay final state *f***

$$\mathcal{T}_r^f = \frac{\frac{1}{2}\sqrt{B_r^e\Gamma_r \cdot B_r^f\Gamma_r}\ e^{i\delta_r}}{W - M_r - i\Gamma_r/2} = \frac{\frac{1}{2}\sqrt{\Gamma_r^e \cdot \Gamma_r^f}\ e^{i\delta_r}}{W - M_r - i\Gamma_r/2}$$

- **In relativistic case, negative energy state (W→ –W) should be included**

$$\mathcal{T}_r^f = [\frac{\frac{1}{2}\sqrt{\Gamma_r^e \cdot \Gamma_r^f}}{W - M_r + i\Gamma_r/2} + \frac{\frac{1}{2}\sqrt{\Gamma_r^e \cdot \Gamma_r^f}}{-W - M_r + i\Gamma_r/2}] = \frac{M_r\sqrt{\Gamma_r^e\Gamma_r^f}}{W^2 - M_r^2 + iM_r\Gamma_r}e^{i\delta_r}$$

Problems in fitting

➢Interference

- **interferential summation of amplitudes with the same channel *f*, but decay from different *r***

$$\mathcal{T}^f_{res} = \sum_r \mathcal{T}^f_r$$

- **non-interferential summation of different decay channels *f***

$$|\mathcal{T}_{res}|^2 = \sum_f |\mathcal{T}^f_{res}|^2$$

- **inclusive resonant cross section is expressed by the form of R value**

$$R_{res} = \frac{\sigma_{res}}{\sigma^0_{\mu\mu}} = \frac{12\pi}{s}|\mathcal{T}_{res}|^2$$

➢Continuous background (polynomial)

$$R_{con} = C_0 + C_1(W - 2M_{D^\pm}) + C_2(W - 2M_{D^\pm})^2$$

➢Energy-dependent hadronic width (potential model in quantum mechanics)

$$\Gamma^{had}_r(W) = \frac{2M_r}{M_r + W}\sum_f \Gamma^f_r(W) \qquad \Gamma^f_r(W) = \hat{\Gamma}_r \sum_L \frac{Z^{2L+1}_f}{B_L}$$

➢Objective function in fitting

$$\chi^2 = \sum_i \frac{[f_c\widetilde{R}_{exp}(W_i) - \widetilde{R}_{the}(W_i)]^2}{[f_c\Delta\widetilde{R}^{(i)}_{exp}]^2} + \frac{(f_c - 1)^2}{\sigma_c^2} \xrightarrow{\text{convergence}} \boxed{\begin{array}{c}\textbf{updated}\\ M\ \Gamma_{ee}\ \Gamma_{tot}\ \delta\\ \text{R values}\end{array}}$$

$$\widetilde{R}_{exp} = \frac{N^{obs}_{had} - N_{bg}}{\sigma^0_{\mu\mu}L\epsilon_{trg}\epsilon_{had}} \qquad \widetilde{R}_{the} = (1 + \delta_{obs})R_{the}$$

Resonance parameters

		$\psi(3770)$	$\psi(4040)$	$\psi(4160)$	$\psi(4415)$
M (MeV/c^2)	PDG2004	3769.9±2.5	4040±10	4159±20	4415±6
	PDG2006	3771.1±2.4	4039±1	4153±3	4421±4
	CB (Seth)	—	4037±2	4151±4	4425±6
	BES (Seth)	—	4040±1	4155±5	4455±6
	BES (this work)	3772.0±1.9	4039.6±4.3	4191.7±6.5	4415.1±7.9
Γ_{tot} (MeV)	PDG2004	23.6±2.7	52±10	78±20	43±15
	PDG2006	23.0±2.7	80±10	103±8	62±20
	CB (Seth)	—	85±10	107±10	119±16
	BES (Seth)	—	89±6	107±16	118±35
	BES (this work)	30.4±8.5	84.5±12.3	71.8±12.3	71.5±19.0
Γ_{ee} (keV)	PDG2004	0.26±0.04	0.75±0.15	0.77±0.23	0.47±0.10
	PDG2006	0.24±0.03	0.86±0.08	0.83±0.07	0.58±0.07
	CB (Seth)	—	0.88±0.11	0.83±0.08	0.72±0.11
	BES (Seth)	—	0.91±0.13	0.84±0.13	0.64±0.23
	BES (this work)	0.22±0.05	0.83±0.20	0.48±0.22	0.35±0.12
δ (degree)	BES (this work)	0	130±46	293±57	234±88

Notice : **mass of ψ(4160) *M* ~ 4155 → 4191 MeV ;**

leptonic widths of ψ(4160) and ψ(4415) are smaller than other's results

Resonant structure

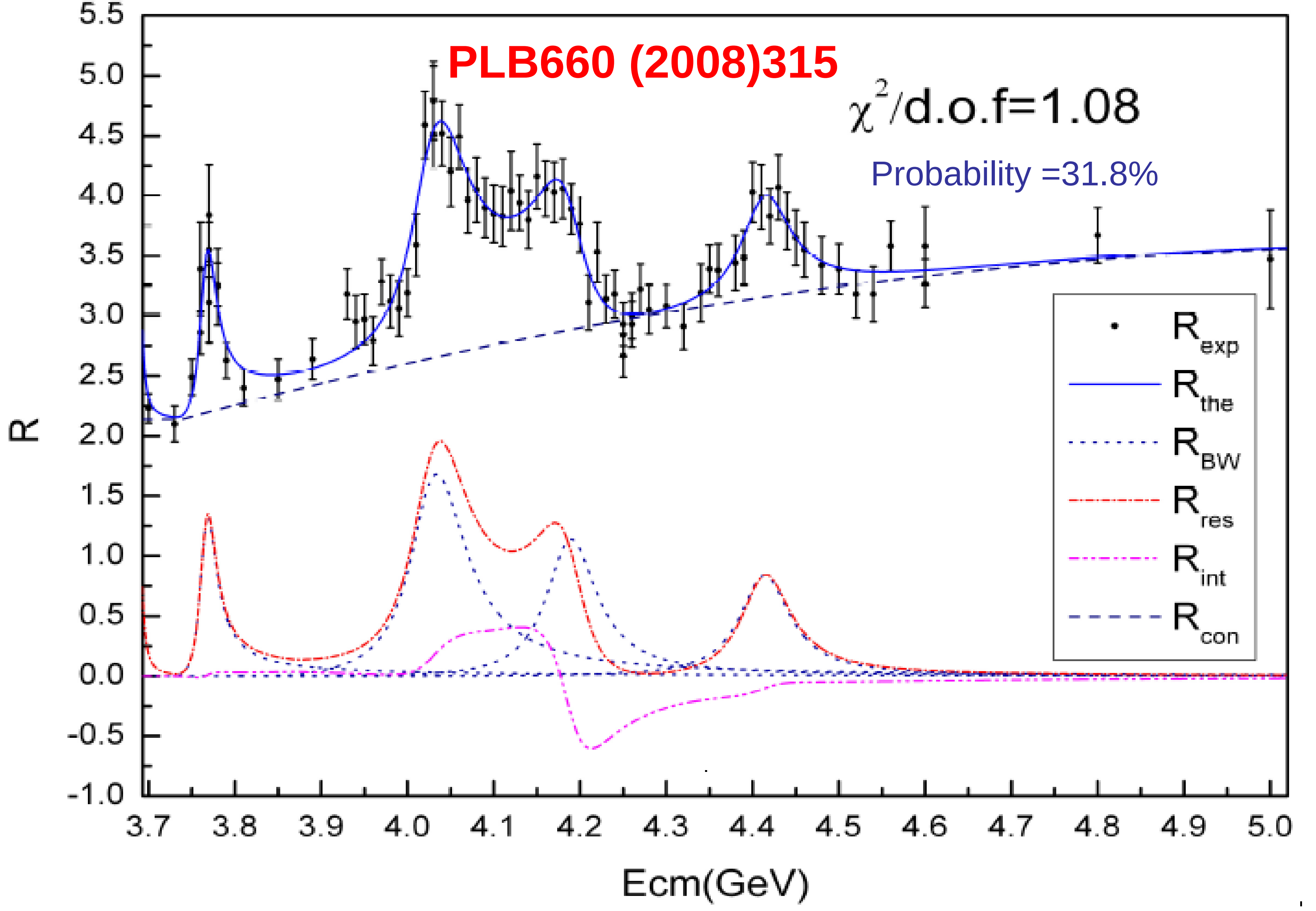

Effect of phase angle

If phase angles are fixed to be $\delta = 0$

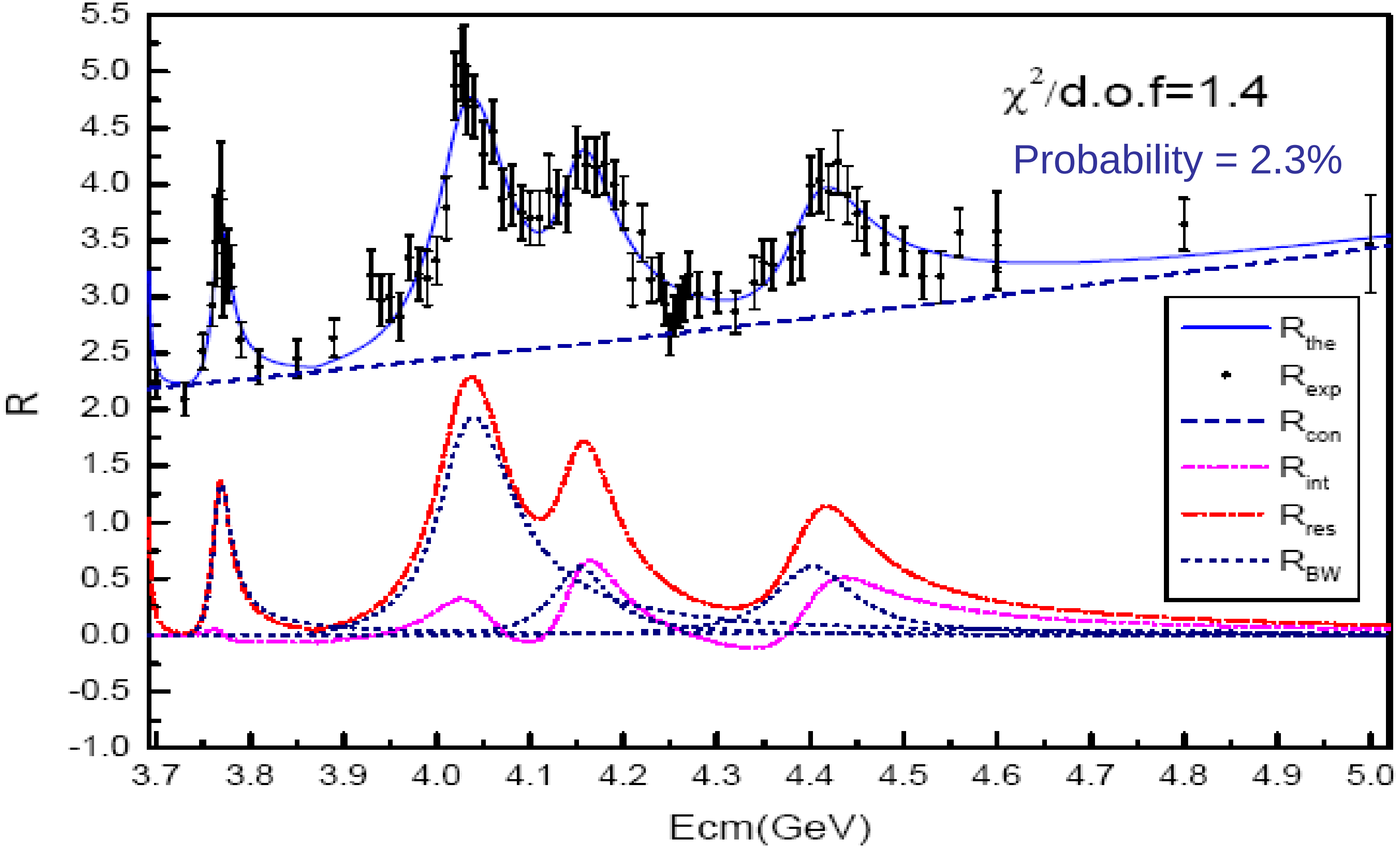

The interferential curve and overall resonances shape for $\delta = 0$ are different from ones for $\delta \neq 0$.

Model dependence

PLB660 (2008) 315

Similar to scheme A but DASP BG used

Similar to scheme A but $\delta = 0$

Parameter	Scheme	$\psi(3770)$	$\psi(4040)$	$\psi(4160)$	$\psi(4415)$
M	A	3772.0 ± 1.9	4039.6 ± 4.3	4191.7 ± 6.5	4415.1 ± 7.9
(MeV/c^2)	B	3772.8 ± 1.9	4046.7 ± 5.2	4198.2 ± 5.4	4425.0 ± 14.1
	C	3772.8 ± 2.0	4048.4 ± 3.2	4156.2 ± 4.4	4405.2 ± 5.7
Γ_{tot}	A	30.4 ± 8.5	84.5 ± 12.3	71.8 ± 12.3	71.5 ± 19.0
(MeV)	B	32.3 ± 9.0	103.6 ± 13.4	61.6 ± 13.8	82.8 ± 26.8
	C	30.8 ± 8.9	109.1 ± 14.9	74.4 ± 14.2	103.8 ± 26.0
Γ_{ee}	A	0.22 ± 0.05	0.83 ± 0.20	0.48 ± 0.22	0.35 ± 0.12
(keV)	B	0.24 ± 0.06	0.93 ± 0.13	0.36 ± 0.27	0.29 ± 0.11
	C	0.23 ± 0.05	1.21 ± 0.17	0.26 ± 0.08	0.37 ± 0.09
δ	A	0	136 ± 46	293 ± 57	234 ± 88
(degree)	B	0	136 ± 42	302 ± 16	245 ± 90
	C	0	0	0	0

Summary

➢R values between 2.20–3.65 GeV are measured with large data samples and improved methods, the errors are decreased. The new measurement agrees with the pQCD prediction within errors.

➢Resonance parameters of high mass charmonia are determined considering the phase angles, interference and energy-dependent width. The model dependences are compared. New results will be helpful to understand the properties (states) of excited charmonia.

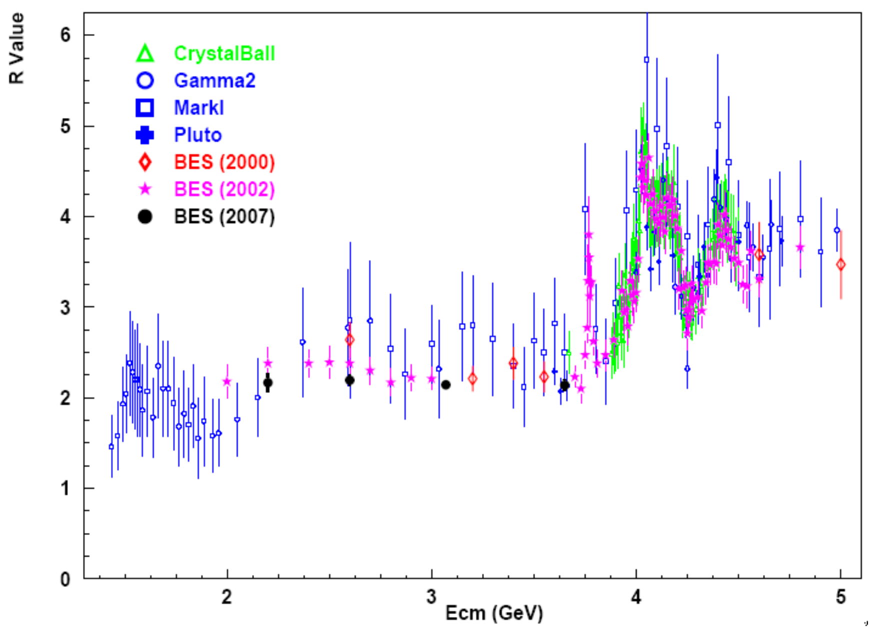

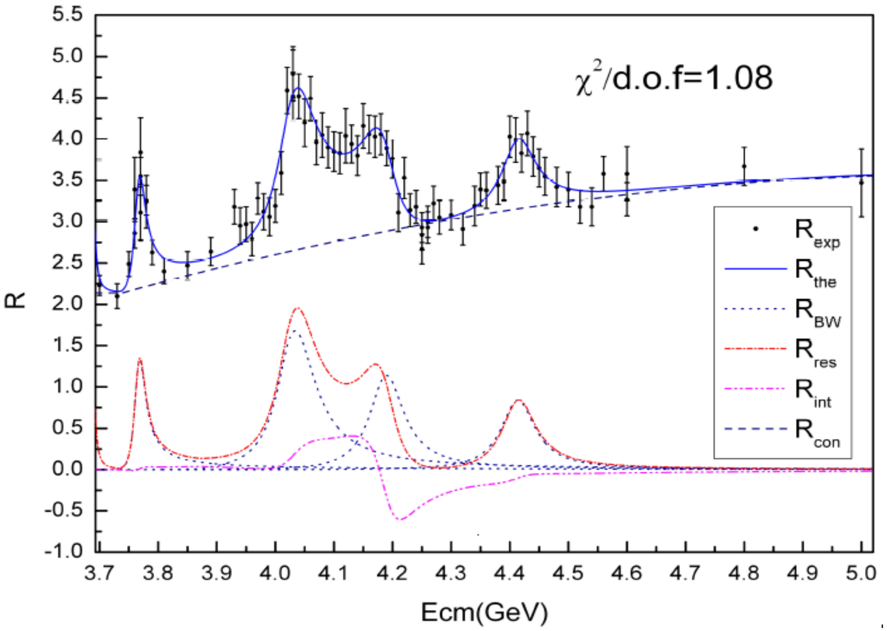

THANK YOU

Tuning of LUARLW parameters

Hadronic efficiency

$$\bar{\epsilon}_{had} = \frac{N^{MC}_{obs}}{N^{MC}_{gen}}$$

the reliability of efficiency depends on the consistency between data and Monte Carlo for all distributions related to hadronic criteria.

There are many free parameters in LUARLW and JETSET, some of them are important for determining the hadronic efficiency, such as

- ✓ **multiplicity distribution for fragmentation hadrons**

$$P_n = \frac{\mu^n}{n!}\exp[c_0 + c_1(n-\mu) + c_2(n-\mu)^2] \quad , \; \mu = \alpha + \beta\exp(\gamma\sqrt{s})$$

- ✓ **ratios of vector/pseudoscalar, strange/normal mesons, baryon/meson**
- ✓ **dynamical parameters b and σ_{pt} in LUND area law**
- ✓ **PARJ(1-3), PARJ(11-17) in JETSET**
- ✓ **……**

The values of the free parameters need to be tuned by comparing the sensitive distributions simulated by LUARLW with data at detector level, and make them to be consistent at all energy points.

Comparisons between data and LUARLW

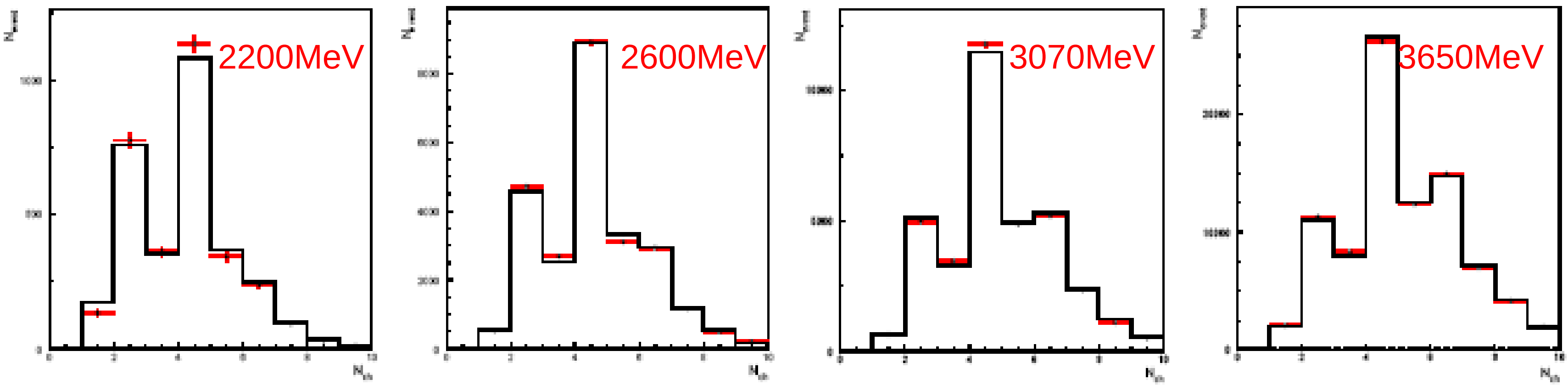

Figure 1: Distribution of the total charged multiplicity.

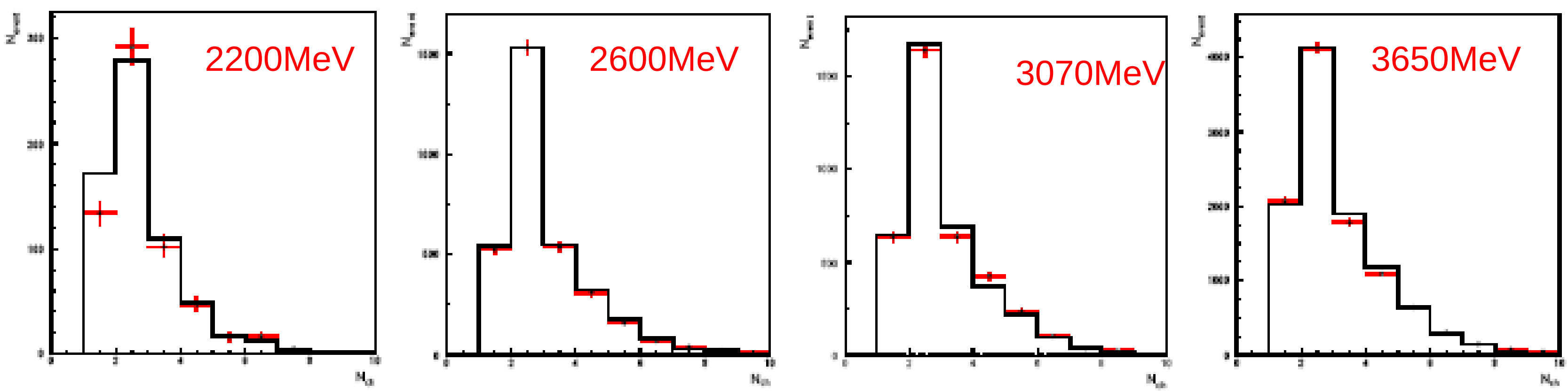

Figure 2: Distribution of charged multiplicity of the events with one good charged track.

Comparisons between data and LUARLW

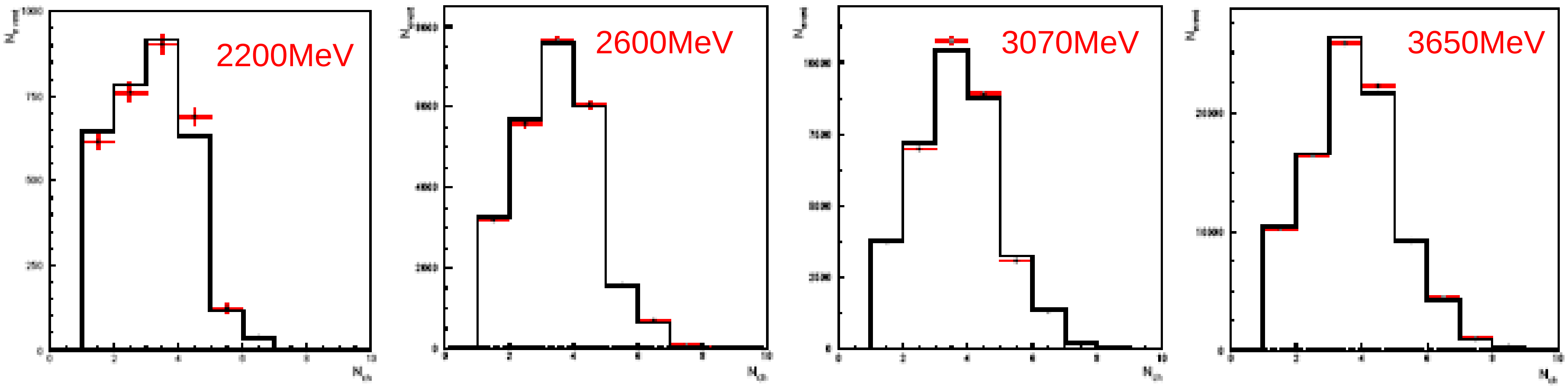

Figure 3: Good charged multiplicity distributions.

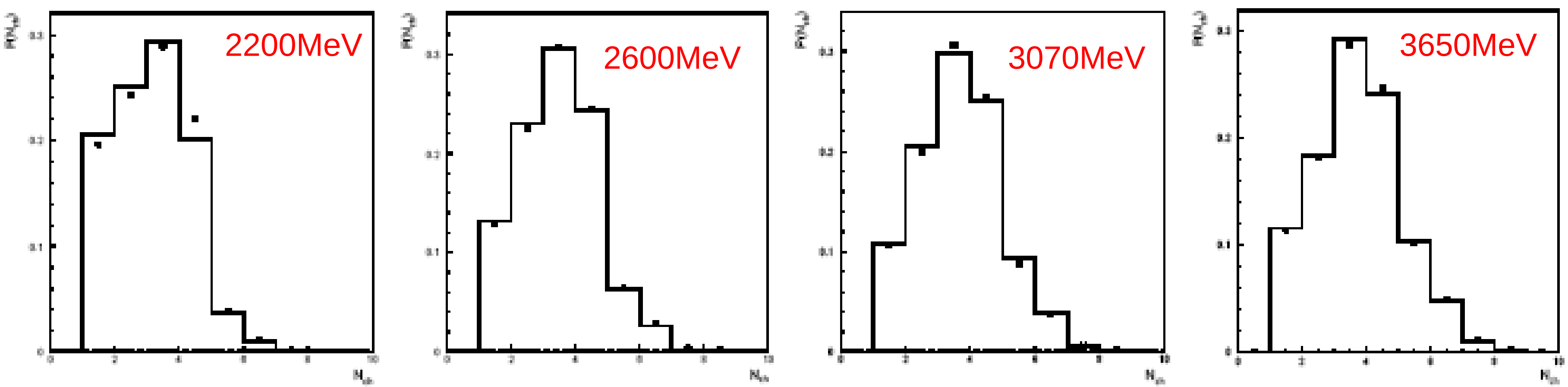

Figure 4: Normalized good charged multiplicity distributions.

Comparisons between data and LUARLW

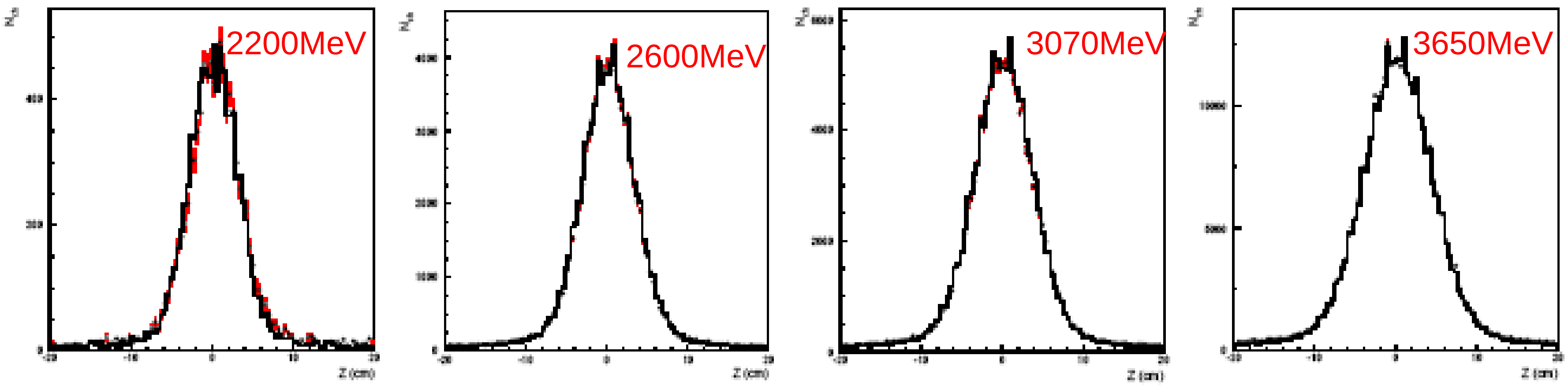

Figure 5: Vertex distribution in z direction for good charged track.

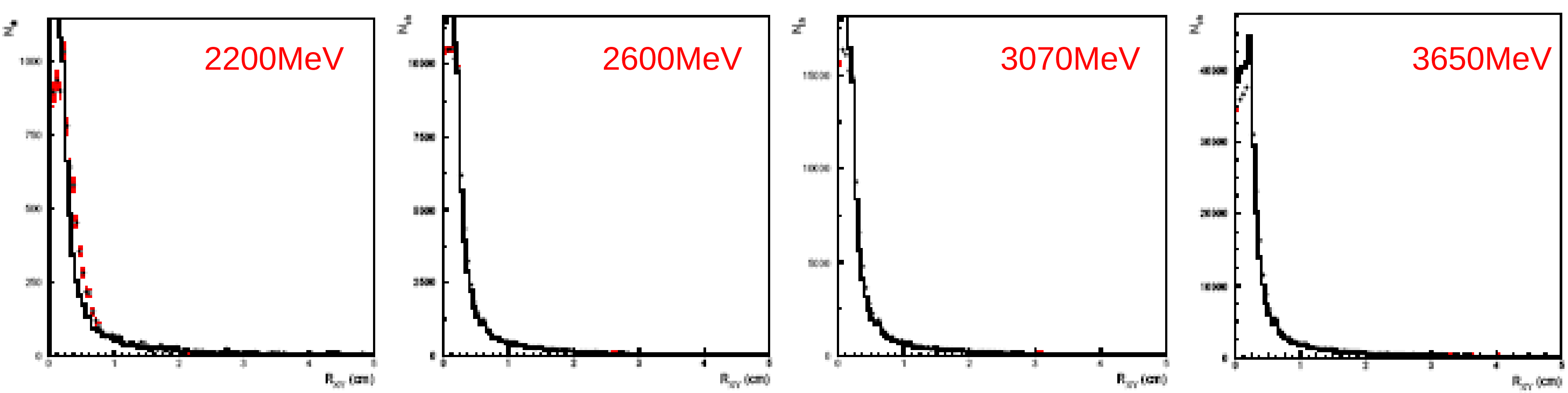

Figure 6: Vertex distribution in $x - y$ plane for good charged track.

Comparisons between data and LUARLW

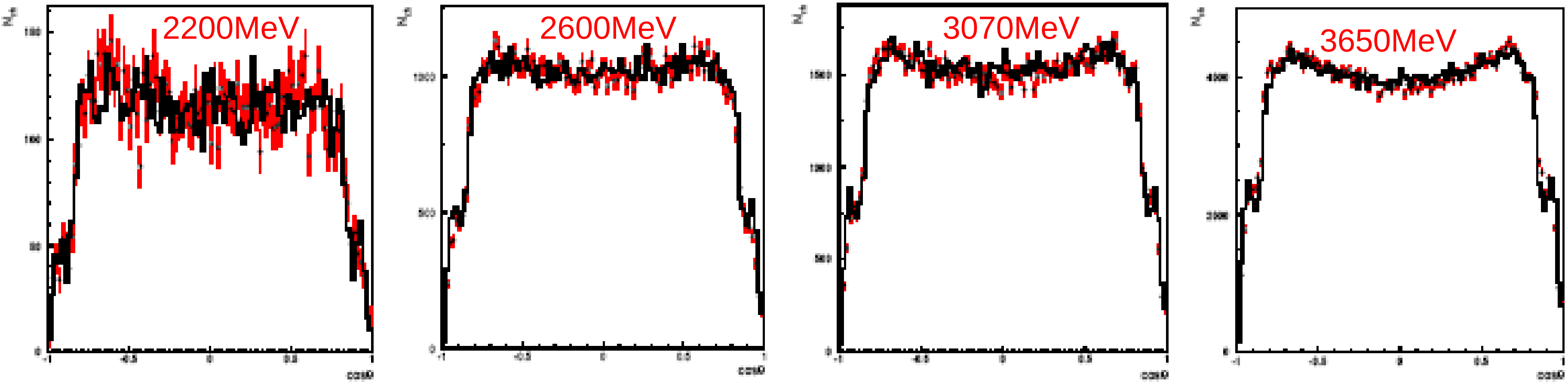

Figure 7: Polar angle $\cos\theta$ in MDC distribution.

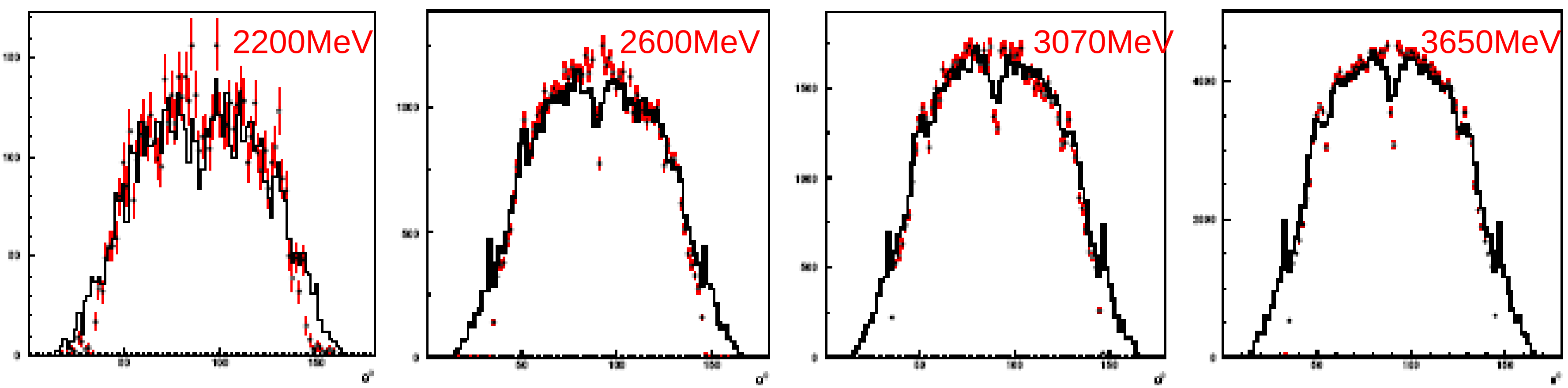

Figure 8: Polar angle $\cos\theta$ in BSC distribution.

Comparisons between data and LUARLW

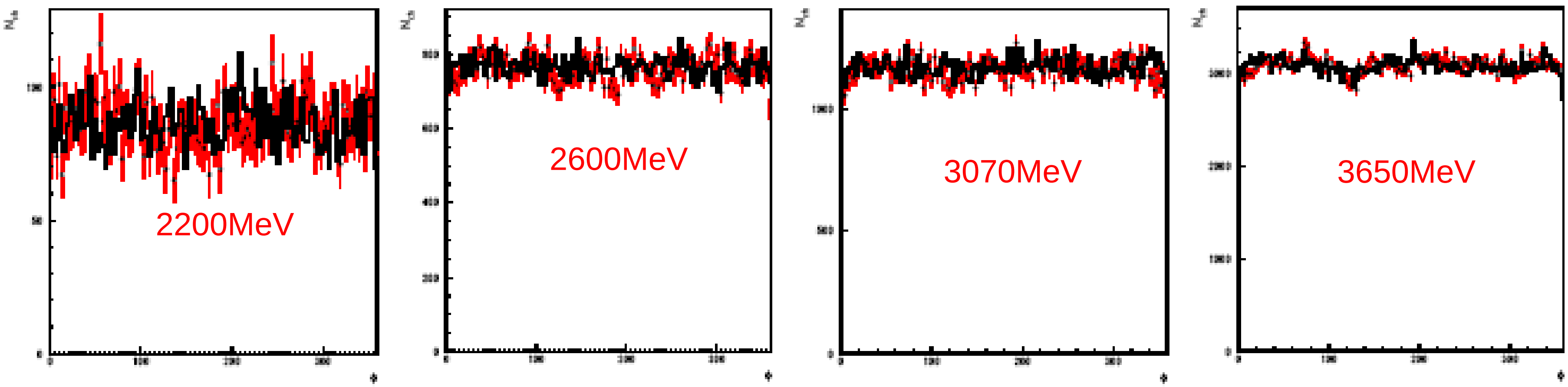

Figure 9: Azimuthal angle ϕ distribution.

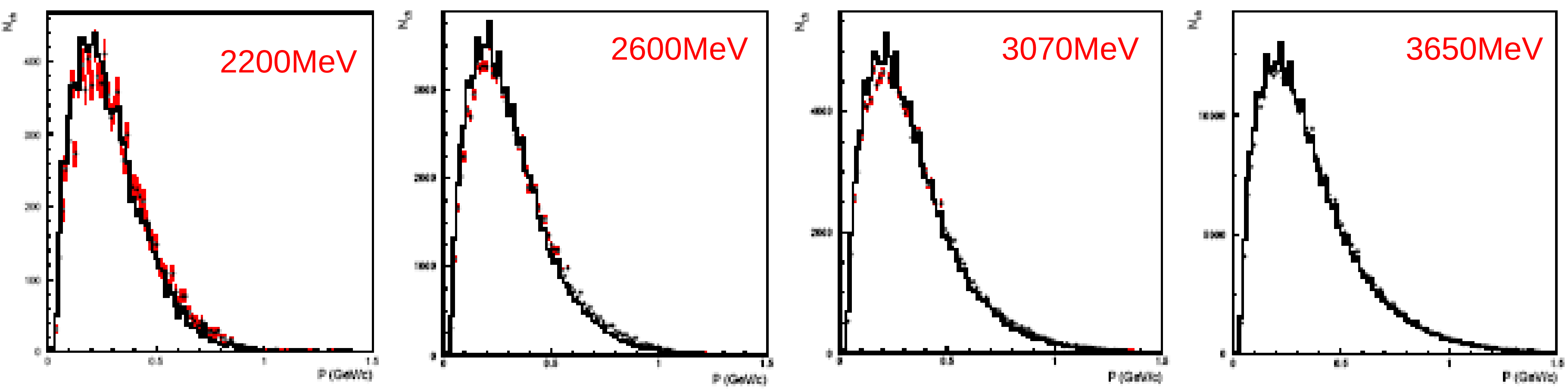

Figure 10: Track momentum p distribution.

Comparisons between data and LUARLW

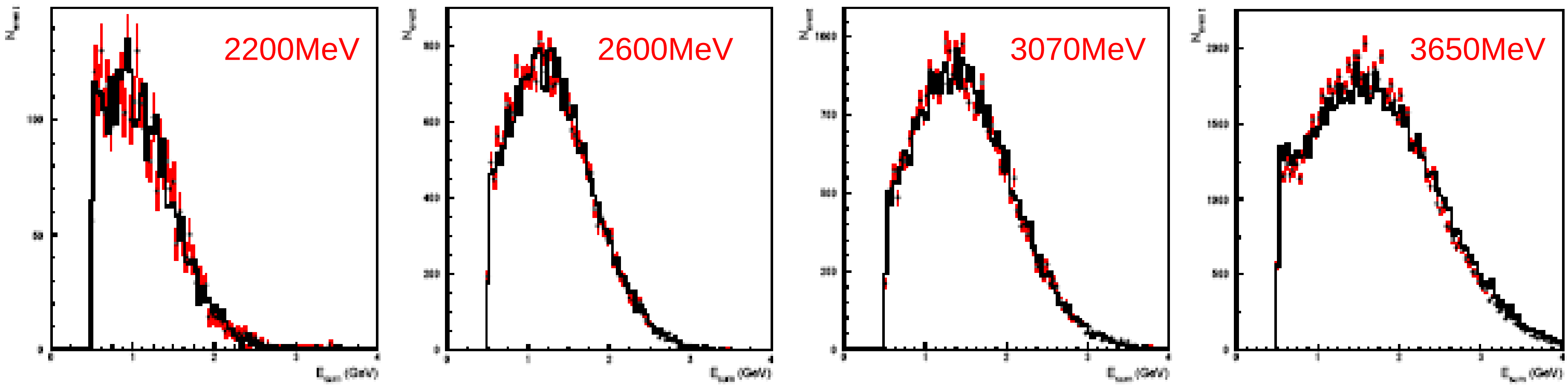

Figure 11: Distribution of deposit energy in BSC.

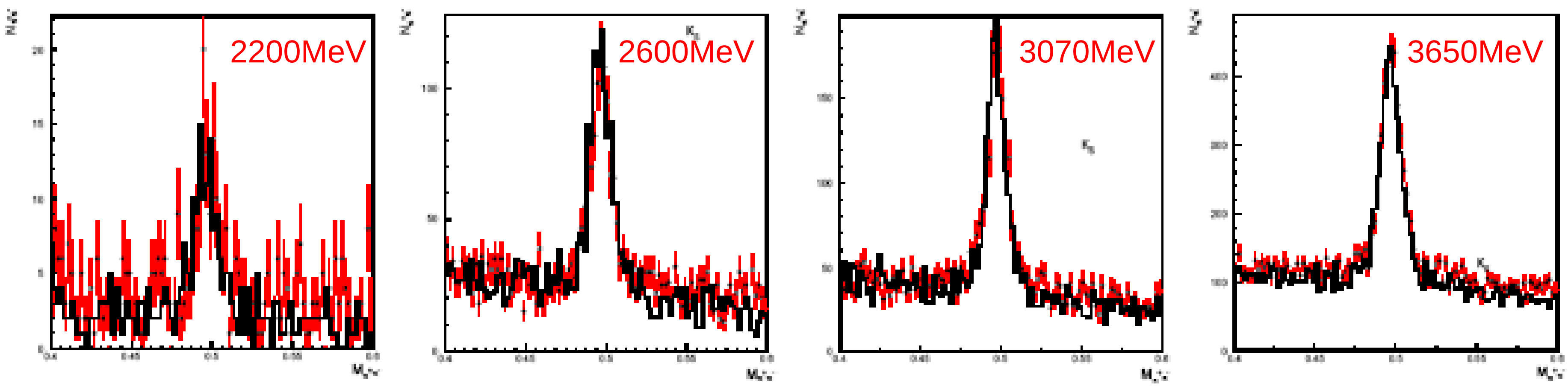

Figure 12: Distribution of invariant mass of $K_S \to \pi^+\pi^-$.

Comparisons between data and LUARLW

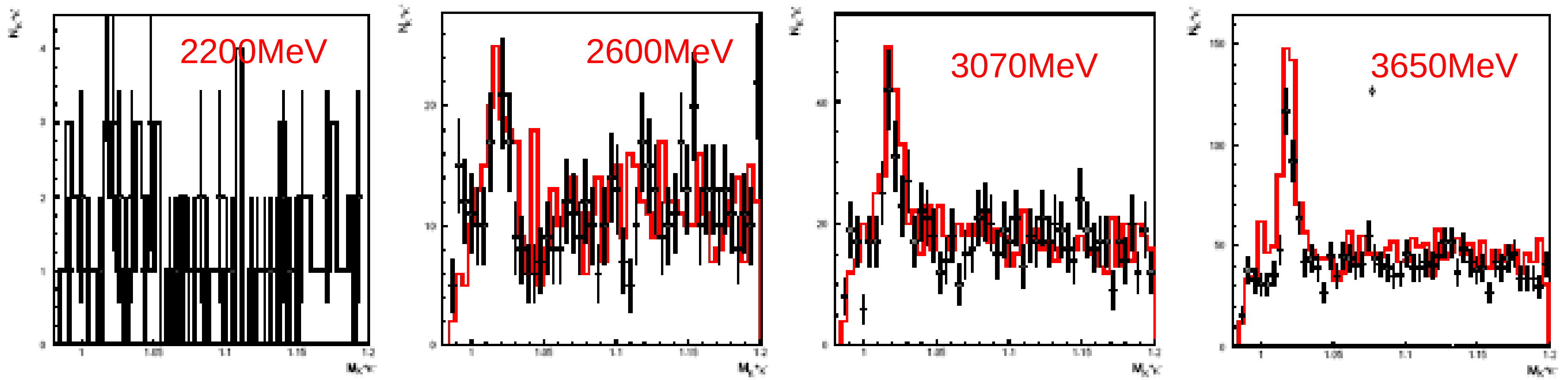

Figure 13: Distribution of invariant mass of $\phi \to K^+K^-$.

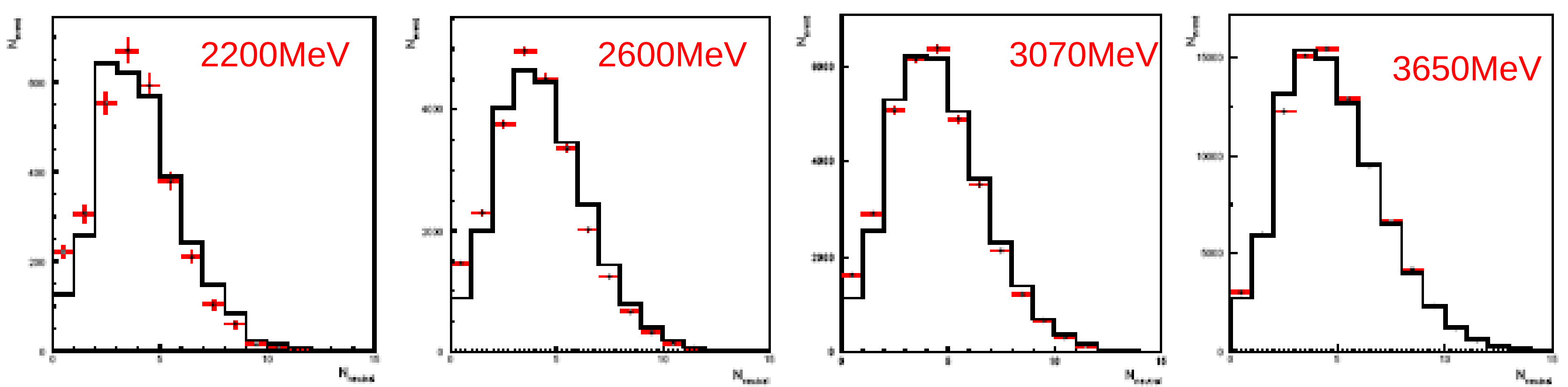

Figure 14: Distribution of the neutral multiplicity.

Comparisons between data and LUARLW

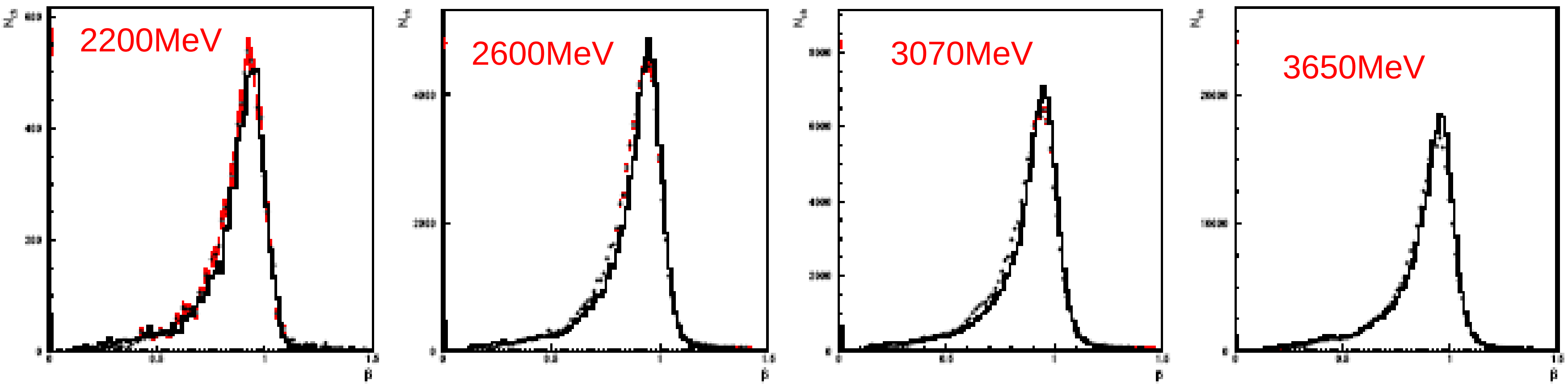

Figure 15: Distribution of the speed of the good charged track.

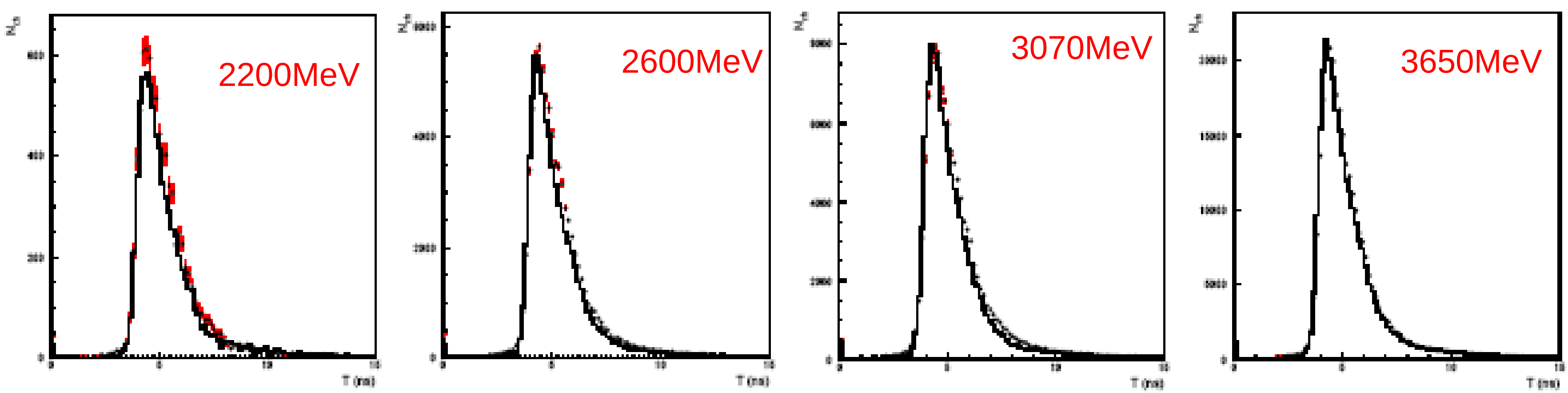

Figure 16: Distribution of the time of flight.

Model dependence

Energy-dependence of hadronic width in effective interaction theory

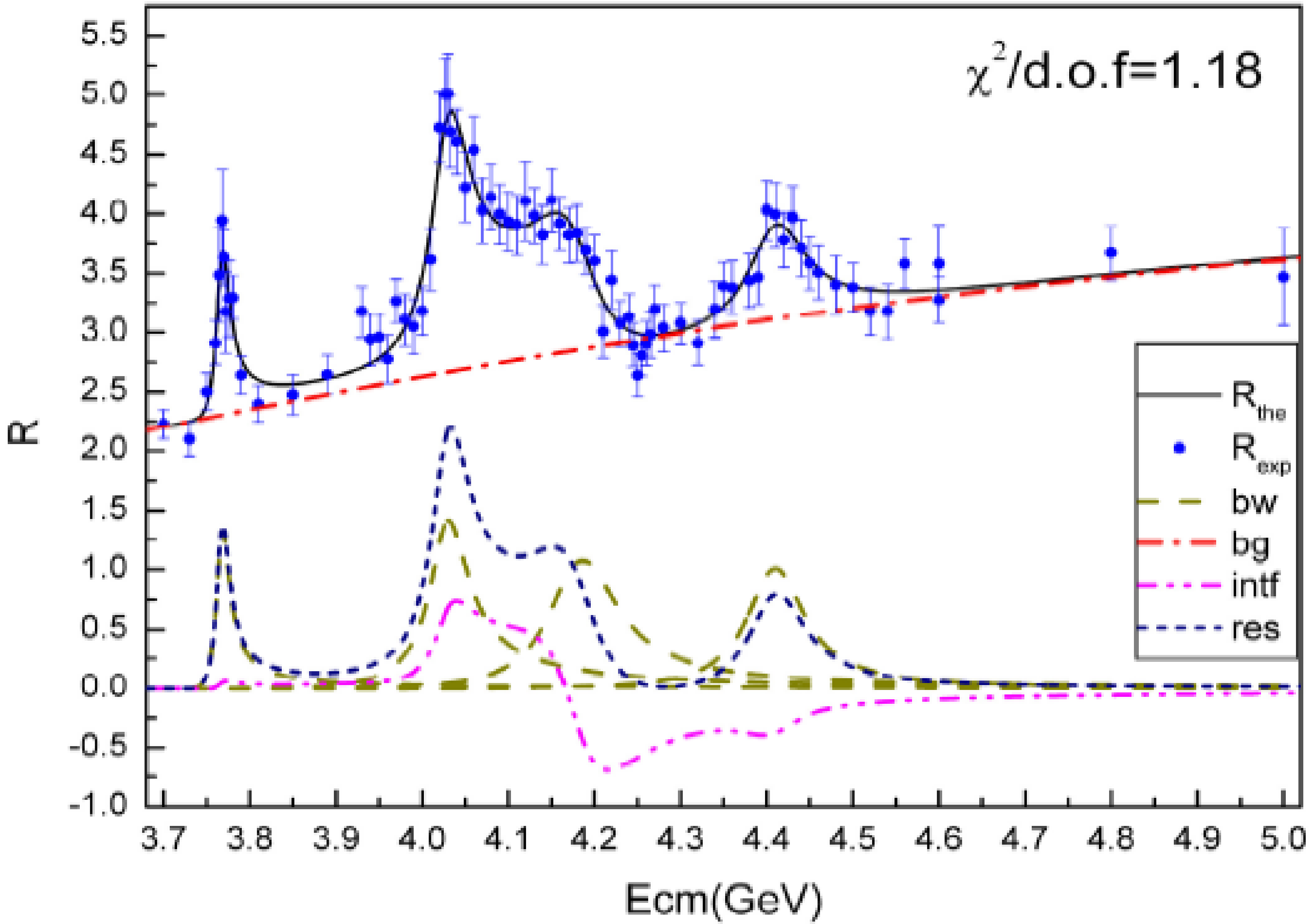

Model dependence

DASP background:

$$\sigma_{con}^{(c)} = \sigma(3.6)\frac{(3.6\ \mathrm{GeV})^2}{s} + \sum_{k=1}^{6} A_k \beta_k^3 \frac{F^2}{s} \quad , \qquad F = \frac{1}{1 - s/(3.1\ \mathrm{GeV})^2}$$

$k =$ $D\bar{D},\ D\bar{D}^*,\ D^*\bar{D}^*,\ D_s\bar{D}_s,\ D_s\bar{D}_s{}^*\ D_s^*\bar{D}_s{}^*$

Effective interaction theory:

$$1^{--} \Rightarrow 0^{-C} + 0^{-C} \quad \mathcal{H}_{eff} = g_1\psi_\mu[(\partial_\mu D)\bar{D}' - D(\partial_\mu \bar{D}')] \qquad (VPP)$$

$$1^{--} \Rightarrow 1^{-C} + 0^{-C} \quad \mathcal{H}_{eff} = g_2\epsilon_{\mu\nu\lambda\sigma}(\partial_\mu\psi_\nu)(\partial_\lambda D_\sigma^*)\cdot\bar{D} \qquad (VVP)$$

$$1^{--} \Rightarrow 1^{-C} + 1^{-C} \quad \mathcal{H}_{eff} = g_4\psi_\mu[(\partial_\mu D_\nu^*)\bar{D}_\nu^* - D_\nu^*(\partial_\mu \bar{D}_\nu^*)] + g_5(\partial_\lambda\psi_\mu)[(\partial_\mu D_\nu^*)(\partial_\nu \bar{D}_\lambda^*) - (\partial_\nu D_\lambda^*)(\partial_\mu \bar{D}_\nu^*)] \qquad (VVV)$$

Energy dependent width:

$$\Gamma_r^f(s) = 8G_r^{PP}\frac{P_f^3}{s} \qquad \Gamma_r^f(s) = 8G_r^{VP}P_f^3 \qquad \Gamma_r^f(s) = 8G_r^{VV}\frac{P_f^3}{s}[3 + \frac{sP_f^2}{M_{D^*}^2 M_{\bar{D}^*}^2}]$$

$G_r^{PP}, G_r^{VP}, G_r^{VV}$ are generalized form factors, free parameters

Determination of α_s

Solving equation: $R_{exp} \pm \sigma_{sts} \pm \sigma_{sys} = R_{QCD}(\alpha_s)$

$\sqrt{s}$(GeV)	$\alpha_s^{(3)}(s)$	$\alpha_s^{(4)}(25\mathrm{GeV}^2)$
2.20	$0.246^{+0.061+0.157}_{-0.059-0.146}$	$0.190^{+0.033+0.076}_{-0.037-0.100}$
2.60	$0.283^{+0.021+0.108}_{-0.021-0.100}$	$0.222^{+0.012+0.058}_{-0.013-0.066}$
3.07	$0.216^{+0.017+0.083}_{-0.017-0.081}$	$0.188^{+0.012+0.057}_{-0.013-0.064}$
3.65	$0.205^{+0.011+0.094}_{-0.011-0.092}$	$0.188^{+0.009+0.075}_{-0.009-0.080}$

$$\bar{\alpha}_s^{(4)}(25\mathrm{GeV}^2) = 0.198^{+0.033}_{-0.038}$$

$$\alpha_s^{(5)}(M_z^2) = 0.113^{+0.010}_{-0.013}$$

PDG2006

$$\alpha_s(M_Z^2) = 0.1170 \pm 0.0012$$